Molecular Crystals and Liquid Crystals

ISSN: 1542-1406 (Print) 1563-5287 (Online) Journal homepage: http://www.tandfonline.com/loi/gmcl20

Conformational and Orientational Determination from Dipolar Couplings in a Weakly Ordering Organic-Based Lyotropic and a Strongly Ordering Thermotropic Liquid Crystal

Maria Enrica Di Pietro, Giuseppina De Luca, Giorgio Celebre, Denis Merlet & Christie Aroulanda

To cite this article: Maria Enrica Di Pietro, Giuseppina De Luca, Giorgio Celebre, Denis Merlet & Christie Aroulanda (2015) Conformational and Orientational Determination from Dipolar Couplings in a Weakly Ordering Organic-Based Lyotropic and a Strongly Ordering Thermotropic Liquid Crystal, Molecular Crystals and Liquid Crystals, 614:1, 39-53, DOI: 10.1080/15421406.2015.1049907

To link to this article: http://dx.doi.org/10.1080/15421406.2015.1049907

Published online: 18 Aug 2015.

Mol. Cryst. Liq. Cryst., Vol. 614: pp. 39–53, 2015

ISSN: 1542-1406 print/1563-5287 online
DOI: 10.1080/15421406.2015.1049907

Taylor & Francis
Taylor & Francis Group

Conformational and Orientational Determination from Dipolar Couplings in a Weakly Ordering Organic-Based Lyotropic and a Strongly Ordering Thermotropic Liquid Crystal

MARIA ENRICA DI PIETRO,[1,2,*] GIUSEPPINA DE LUCA,[1] GIORGIO CELEBRE,[1] DENIS MERLET,[2] AND CHRISTIE AROULANDA[2]

[1]Dipartimento di Chimica e Tecnologie Chimiche, Università della Calabria, Arcavacata di Rende (CS), Italy
[2]Equipe de RMN en milieu orienté, ICMMO, Université Paris-Sud, Orsay, France

A weakly ordering organic-based lyotropic phase and a strongly ordering nematic liquid crystal have been used as NMR media for a parallel study of the conformation and orientational order of the same solute, trans-stilbene. A careful comparison allows to figure out some interesting conclusions on accessibility and precision of the experimental data and reliability and accuracy of the conformational descriptions into these two kinds of mesophases.

Keywords NMR spectroscopy; Dipolar Couplings; Stilbenoids; Liquid crystals; Conformational analysis; Orientational order

Introduction

Since the pioneering work of Saupe and Englert in 1963, [1] liquid crystals proved to be very attractive media for NMR studies of solutes dissolved therein [2–4]. In these media, the anisotropic part of the NMR interactions (chemical shift anisotropy, indirect spin-spin coupling anisotropy, dipolar coupling, and quadrupolar splitting) becomes observable and can give direct access to molecular properties. In particular, the analysis of order, structure and conformational equilibrium of flexible molecules starting from experimental dipolar couplings D_{ij} gained much attention thanks to the plenty of applications and fields of interest [2–5]. For this purpose, many different liquid crystalline phases have been explored, that can be roughly divided depending on the degree of orientational order they induce to the solute.

*Address correspondence to Dr. Maria Enrica Di Pietro, Dipartimento di Chimica e Tecnologie Chimiche, Università della Calabria, via P. Bucci, 87036, Arcavacata di Rende (CS), Italy. E-mail: mariaenrica.dipietro@unical.it

Color versions of one or more of the figures in the article can be found online at www.tandfonline.com/gmcl.

Thermotropic liquid crystals (typically uniaxial nematics) induce a rather strong statistical alignment, with typical values of the solute's orientational order parameters on the order of 10^{-1}–10^{-2} and D_{ij} values from few Hz up to thousands of Hz [6]. Their use as NMR solvents allows to obtain very accurate NMR spectral parameters, which lead to precise information on structure, orientation and conformational distribution [7–8]. The main limitation is the complexity of the spectra, that are characterized by the presence of a very high number of distinct transitions evenly dispersed over a few 10^4 Hz frequency range and by strong second order spectral features. Such spectral complexity limited traditionally their use to highly symmetric molecules with no more than 10 to 12 spins [9–15]. Several strategies have been proposed to help in the spectral analysis and recently automated spectral fitting routines gained some interest [16–17]. Nevertheless, there are severe limitations since they require as a prerequisite a good starting set of parameters or a good estimation of the solute's orientational order.

Aiming at treating more complex molecules of lower symmetry, a wide range of weakly ordering liquid crystalline media has been explored over the years [18–23]. Among those soluble in organic solvents, the most popular are probably the chiral nematic phases made of synthetic homopolypeptides, namely poly-γ-benzyl-*L*-glutamate (PBLG), poly-γ-ethyl-*L*-glutamate (PELG), or poly-ε-carbobenzyloxy-*L*-lysine (PCBLL), dissolved in helicogenic organic solvents [24–27]. Such ordered media were successfully used to determine structural and relative configuration, to measure enantiomeric excesses, to discuss reaction pathways and recently to investigate the conformational equilibrium of small drugs [28–40]. In such phases the solute's orientational order parameter is within the range 10^{-3} to 10^{-5} [6]. The advantageous consequence is that the orientation-dependent NMR interactions are significantly reduced (the D_{ij} values are of Hz or tens of Hz) so that the spectral quality of high-resolution NMR spectra is generally retained. On the other hand, note that only the largest dipolar interactions can be practically simply measured. For the spectral edition of smaller couplings, (specifically) designed NMR experiments as *J*-resolved type and E.COSY methods must be developed and used [28, 41–44]. However, the percentage error measured on D_{ij} with small magnitude is, for the same absolute error, generally greater than in thermotropic spectra. These factors may compromise the level of precision in the subsequent analysis.

From the above, it is clear why the choice between thermotropic and lyotropic liquid crystals as NMR solvents for structural and conformational studies is currently mainly driven by the size and symmetry of the target molecule. The balance between difficulty in spectral analysis *versus* extent and precision/accuracy of the data set should be taken into account: small symmetric molecules/spin systems are suitable for strong alignment in thermotropic phases to give valuable long-range interactions and consequently a detailed orientational analysis and an accurate structural and conformational elucidation; information on more complex molecules with lower symmetry can be obtained by using weakly ordering media in order to solve specific constitutional, configurational and/or conformational questions. In this work, we present for the first time a conformational and orientational study of the same solute, *trans*-diphenylethene, commonly known as *trans*-stilbene (*t*-St), in both a nematic highly ordering and a homopolypeptide lyotropic weakly ordering liquid crystal. *t*-St is the simplest member of the stilbenoid family, including several natural and synthetic compounds with multiple biological activities [45–55] and technological properties [56–59]. The symmetric structure and conformational distribution characterized by two coupled rotations make *t*-St a suitable intermediate point for a parallel study in thermotropic and lyotropic phases. In a previous work [10] we reported the experimental analysis of its ^{1}H NMR spectrum in the thermotropic nematic liquid crystals ZLI1132 and we described

its conformational distribution. Here we present a similar study in a lyotropic liquid crystal composed of PBLG dissolved in THF-d_8 and we compare orientational and conformational results from both phases. We present first a brief overview of the methodology, including the basic theoretical tools required for the interpretation of NMR data. In both phases we used the AP-DPD approach [60–61] that is well-tested for thermotropic systems but few examples have been reported so far for weakly ordered samples [28, 62–63]. The strategy is then applied to the case of *t*-St in the PBLG/THF-d_8 phase and the conformational results in the two phases are discussed. The final aim is to evaluate whether or not a reliable conformational description can be obtained starting from a limited and less accurate set of NMR data extracted for the weakly ordered sample. To complete the comparison, some conclusions about the different orientational behavior in the two phases with a different degree of order are also drawn.

Method

The structural, conformational and orientational analysis presented in this study requires the knowledge of experimental NMR data, namely the observed dipolar couplings D_{ij}^{obs} between the i-th and j-th magnetically active nuclei of the studied molecule. These D_{ij}^{obs} are quantities partially averaged over all the relevant molecular motions (namely, internal vibrations and rotations and whole reorientational motions). They depend on the spin-spin distance and on the mean orientation of the internuclear vectors with respect to the external magnetic field. As a consequence, they represent a valuable probe sensitive to the long-range constraints of even spatially remote parts of molecules and can thus give insight into the orientational behavior and conformational distribution of organic compounds. Within some approximations, the D_{ij}^{obs} for a flexible molecule can be written as follows: [10, 28]

$$\mathrm{D}_{ij}^{obs} \approx \left(\frac{3cos^2\omega - 1}{2}\right) \times \frac{2}{3} \cdot \frac{Z_{iso}}{Z} \int P_{iso}\left(\{\phi\}\right) W\left(\{\phi\}\right) \sum_{\zeta\xi} S_{\zeta\xi}\left(\{\phi\}\right) D_{ij,\zeta\xi}\left(\{\phi\}\right) d\{\phi\} \tag{1}$$

where ω is the angle between the external magnetic field B_0, defining the Z direction in the laboratory frame, and $\hat{n}$, the director of the mesophase; $\{\phi\}$ is the set of internal angles defining the conformation. Z and Z_{iso} are proper normalization constants. The term $P_{iso}(\{\phi\})$ defines the probability distribution of the solute in a "virtual" conventional isotropic liquid sharing, at the experimental temperature, the same physical properties of the liquid-crystalline solvent, with the exception of its ability to induce a solute ordering. It must be stressed here that $P_{iso}(\{\phi\})$ is actually the pertinent conformational target. The $D_{ij,\zeta\xi}(\{\phi\})$ are the Cartesian components, given in the molecular frame, of the D_{ij} dipolar coupling tensor between the i-th and the j-th nucleus. $W(\{\phi\})$ can be written as follows:

$$W\left(\{\phi\}\right) = \int exp\left[-U_{ext}\left(\beta, \gamma, \{\phi\}\right)/k_B T\right] \times sin\beta d\beta d\gamma \tag{2}$$

where k_B is the Boltzmann constant and T the absolute temperature. $U_{ext}(\beta, \gamma, \{\phi\})$ is the solute-solvent purely anisotropic orientational potential that contains the orientational-conformational interdependency.

Finally, the terms $S_{\zeta\xi}(\{\phi\})$ are the conformationally dependent solute orientational order parameters, constituting the real symmetric traceless Saupe ordering matrix, and they can be expressed as: [64–65].

$$S_{\zeta\xi}(\{\phi\}) = \frac{1}{W(\{\phi\})} \int \frac{3\cos\theta_\zeta \cos\theta_\xi - \delta_{\zeta\xi}}{2} exp\left[-U_{ext}(\beta, \gamma, \{\phi\}) / k_B T\right] \times \; sin\beta d\beta d\gamma \tag{3}$$

where $cos\theta_\zeta$ is the direction cosine of the director with the ζ molecular axis and $\delta_{\zeta\xi}$ is the Kronecker delta function.

The main consequence of eq. (1) is that a theoretical model describing both the conformation-orientation dependent anisotropic potential and $P_{iso}(\{\phi\})$ must be adopted. In this work, we used the so-called AP-DPD approach, a combination of the Additive Potential model [60], for the treatment of the ordering interactions, with the Direct Probability Description [61] of the torsional distribution $P_{iso}(\{\phi\})$ (for an extensive theoretical treatment see refs 10 and 11).

Within the AP model, the potential $U_{ext}(\beta, \gamma, \{\phi\})$ can be described by a spherical harmonics expansion whose $\{\phi\}$-dependent coefficients can be conveniently constructed as a sum of $\{\phi\}$-independent tensorial contributions $\varepsilon^j_{2,p}$ from each rigid fragment j of the molecule [66]. In practice, the $\varepsilon^j_{2,p}$are unknown quantities whose values are adjusted to obtain the best agreement with the experimental data. As in ref. 10, three $\varepsilon^j_{2,p}$ are required for *t*-St: $\varepsilon^R_{2,0}$ and $\varepsilon^R_{2,2}$, for each ring, and $\varepsilon^{H6-C=C-H7}_{2,0}$, for the vinyl group.

The DPD approach accounts for the torsional distribution and its strength is in modelling the $P_{iso}(\{\phi\})$ in terms of Gaussian functions. *t*-St possesses two internal rotational degrees of freedom ϕ_1 and ϕ_2 (Fig. 1) that give two most stable conformations [10]: a disrotatory, propeller-like conformation with C_2 point group, where the rings are tilted at the same angle with respect to the *ene* plane ($\phi_1 = \phi_2$) and a conrotatory conformation with C_i point group, where the rings are parallel to each other ($\phi_1 = -\phi_2$).

The torsional probability distribution $P_{iso}(\phi_1, \phi_2)$ can be then directly modelled as a sum of bidimensional Gaussian functions by using the following general form already applied for *t*-St and 4,4'-dichloro-*trans*-stilbene: [9–10].

$$P_{iso}(\phi_1, \phi_2) \propto \sum_{\text{over the different } C_x - \text{ symmetry structures}} \frac{A_{C_x}}{n_{C_x}} \cdot \sum_{k=1}^{n_{C_x}} exp\left[-\left(\frac{sin^2\left(\phi_1 - \left(\phi_1^{max}\right)^k_{C_x}\right)}{2h_1^2} + \frac{sin^2\left(\phi_2 - \left(\phi_2^{max}\right)^k_{C_x}\right)}{2h_2^2}\right)\right] \tag{4}$$

where n_{C_x} is the number of rotamers belonging to the C_x point group and A_{C_x} is the global relative weight of the C_x structures (so that $\sum_{(\text{over all the } C_x)} A_{C_x} = 1$). $(\phi_i^{max})^k_{C_x}$ represents, for the i-th torsion, the twist angle corresponding to the k-th of the the n_{C_x} most probable conformations with C_x symmetry. Finally, $h_1$and h_2 give the width at half maximum height along each dimension of the bidimensional Gaussians.

The practical application of this theoretical apparatus for the determination of the conformational distribution and orientational order is performed through a dedicated home-made software called AnCon [67]. Once fixed the molecular geometry, the calculations are carried out by fitting the set of independent D^{obs}_{ij} against a set of calculated dipolar couplings, while iterating on a pertinent number of unknowns. Such unknowns can be: orientational parameters, represented by the set of $\varepsilon^j_{2,p}$; conformational parameters, represented by the

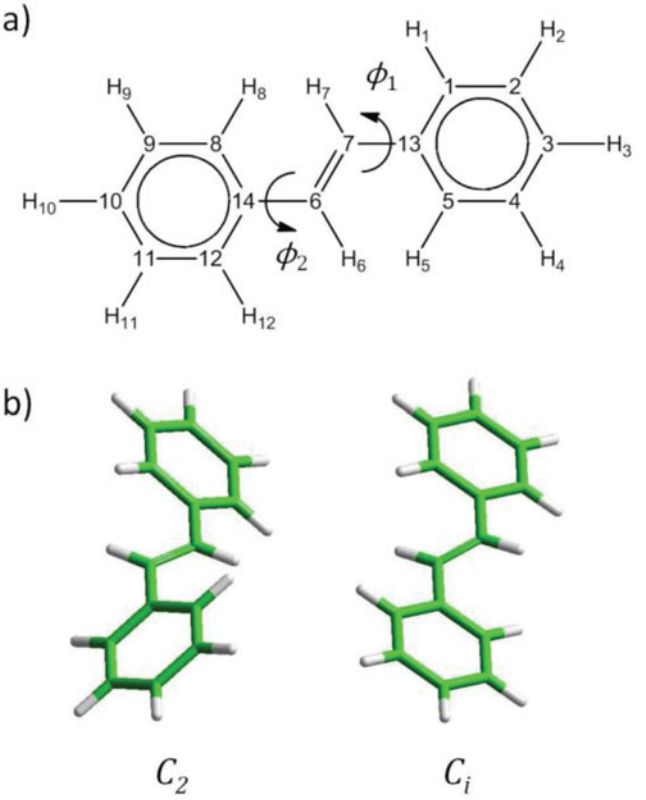

Figure 1. **(a)** Topological structure, numbering and torsional angles and **(b)** minimum energy conformers with corresponding point groups of *trans*-stilbene (*t*-St).

terms A_{C_x}, $(\phi_i^{max})_{C_x}^k$ and h_i of eq. (4); geometrical parameters. At the end of the convergent process, the back-calculated values of the dipolar couplings, D_{ij}^{calc}, are compared to the experimental ones, until the smallest value for the RMS (root mean square) error is obtained (RMS $= \{M^{-1} \sum_{i<j} [D_{ij}^{obs} - D_{ij}^{calc}]^2\}^{\frac{1}{2}}$, M being the number of independent couplings) and a good agreement between D_{ij}^{obs} and D_{ij}^{calc} is reached.

NMR Spectral Analysis of *trans*-Stilbene in PBLG/THF-d_8

Experimentally speaking, what is directly measured from the anisotropic spectra is the total coupling constant, defined as $|T_{ij}^{obs}| = |J_{ij}^{iso} + 2D_{ij}^{obs}|$ (for i and j non-equivalent nuclei, neglecting as usually the anisotropy of indirect coupling [68–69]). Hence, in order to edit the target D_{ij}^{obs}, one has to measure the set of scalar couplings J_{ij}^{obs} from the NMR spectra of the isotropic sample and the set of total couplings T_{ij}^{obs} from the spectra of the anisotropic sample. The set of D_{ij}^{obs} is then given by $D_{ij}^{obs} = [\pm T_{ij}^{obs} - (\pm J_{ij}^{iso})]/2$. For *t*-St we prepared (a) an isotropic sample by diluting *t*-St (36.2 mg) in THF-d_8 (665.5 mg) and (b) an anisotropic sample by dissolving *t*-St (47.2 mg) in a chiral nematic liquid-crystalline (LC) phase made of PBLG (92.5 mg, DP = 743) dissolved in THF-d_8 (483.6 mg), using standard procedure described in literature [26]. The resulting *o.d.* 5 mm NMR tube was

centrifuged back and forth until an optically homogeneous birefringent phase was obtained. *t*-St and PBLG were purchased from Sigma Aldrich, while THF-d_8 from Eurisotop. All the chemical compounds were used without further purification. To edit a set of experimental dipolar couplings as large as possible, multiple homo- and heteronuclear experiments were carried out on both samples. All spectra were recorded at 298 K on a liquid high-resolution Bruker Avance 500 MHz spectrometer (11.74 T) equipped with a TBO probe and a standard variable-temperature unit BVT-3000. Spectral assignment of the peaks was performed by 1D ^{1}H, ^{13}C, ^{13}C-{^{1}H} spectra and 2D ^{1}H-^{1}H COSY, ^{1}H-^{13}C HSQC and HMBC correlation experiments, while homo- and heteronuclear *J*-resolved and SERF [70] experiments were used to extract ^{1}H-^{1}H and ^{1}H-^{13}C scalar and total couplings. Unfortunately, spectra were not well resolved and the superposition of signals from three of the four chemically equivalent protons (see the 1D ^{1}H broadband spectrum in Fig. 2a) made it complicated to accurately measure and unambiguously assign the observed couplings. However, some tricks were exploited and, as an example, Fig. 2 reports the ^{1}H-^{1}H *J*-resolved spectrum (b) and the SERF-like spectrum resulting from the application of a semi-selective pulse selecting *meta*, *para* and ethylenic protons and excluding *ortho* protons (c). Signal from H_3 gives a triplet of triplets in the *J*-resolved spectrum, from which two couplings can be measured. A simple conclusion is these total couplings correspond to H_2-H_3 and H_1-H_3, that are the nearest nuclear pairs. Looking at the SERF spectrum, where only couplings between H_3, H_2 and H_7 should be present (H_1 is the only proton having chemical shift far enough from the others to be excluded from the semi-selective pulse) a similar spectral pattern is observed for H_3. This means that the total coupling T_{13} is not observed and H_3 is coupled to H_6 and H_7 with a similar coupling constant. To be sure that H_3, H_2 and H_7 have been exclusively selected by the soft pulse, consider that (*i*) no signal at 7.56 ppm (the resonance frequency of H_1) is present in the SERF 2D spectrum, and (*ii*) F_2 projection after tilt gives for H_2 a singlet in the *J*-resolved spectrum (all couplings appear in the F_1 dimension) and a doublet in the SERF spectrum (after tilt of the 2D map, couplings among selected protons appear only in the F_1 dimension, while coupling with H_1 is refocused and appears in the direct dimension).

Finally, 13 independent D_{ij}^{obs} (6 D_{HH} and 7 D_{CH}) were collected, and in particular 7 for the phenyl ring, 2 for the *ene* group and 4 between each ring and the *ene* group (Table 1). It is worth noting that the number of dipolar couplings extracted for this sample is lower than the set of D_{HH} set extracted from a single 1D ^{1}H spectrum in the thermotropic nematic phase ZLI1132 (19 independent values and in particular 6 between each ring and the central *ene* group and 6 between the two rings) [10]. From the experimental viewpoint, the presence of elements of symmetry in the spin system represents a big advantage for highly ordering systems, since they simplify the spectrum. Contrarily, when the same solute is dissolved in weakly aligning media, molecular symmetry induce a reduction in the number of independent couplings one can hope to obtain.

Conformational Results for *trans*-Stilbene in PBLG/THF-d_8 and Comparison with ZLI1132

Even though not very extended, the set of experimental D_{ij}^{obs} extracted for *t*-St dissolved in PBLG/THF-d_8 allows a conformational analysis through the software AnCon. The purpose here is not merely the description of the potential surface and the determination of the lowest energy conformers, but also the comparison with results obtained in the ZLI1132 liquid

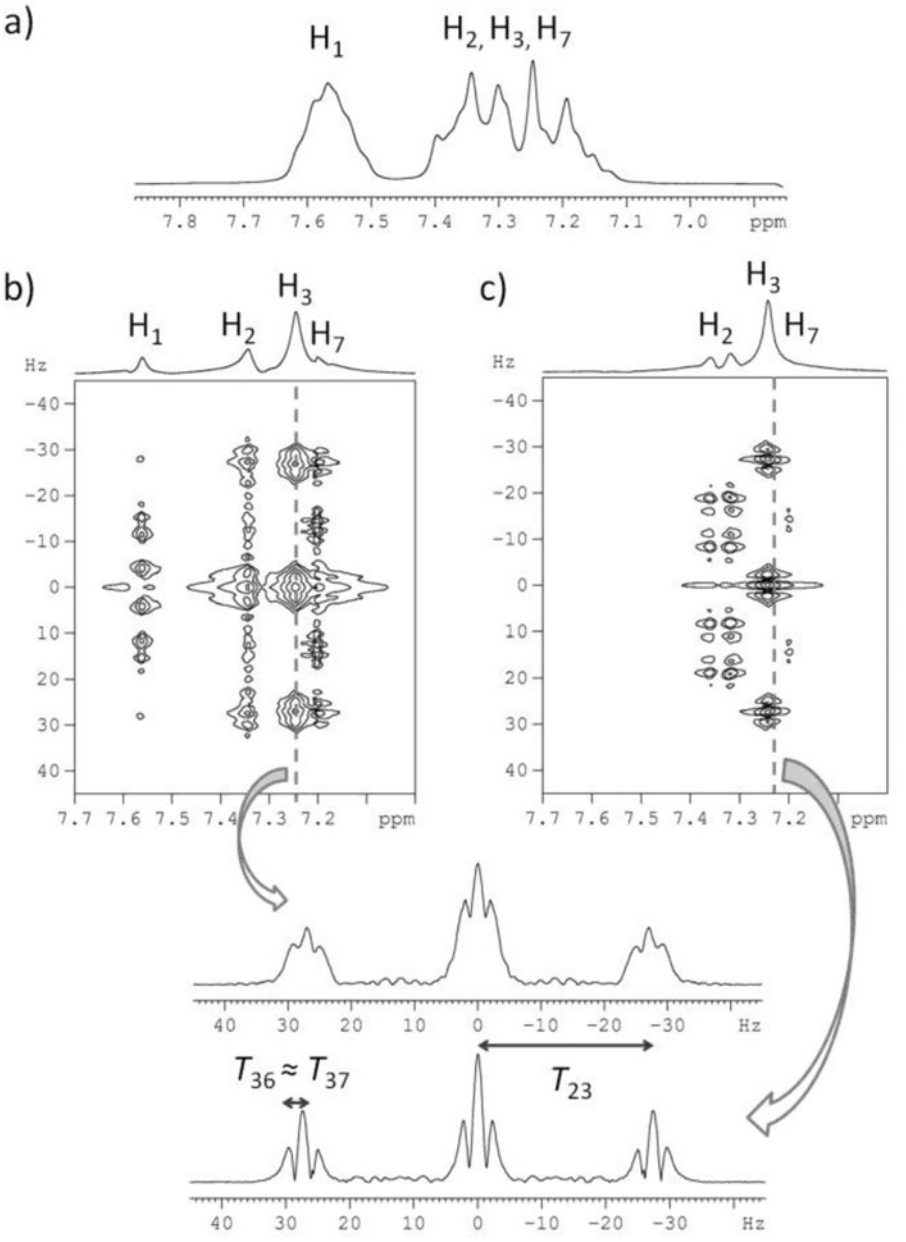

Figure 2. **(a)** 1D ^{1}H broadband excitation spectrum recorded on *trans*-stilbene in PBLG/THF-d_8 at 298 K. **(b)** Tilted ^{1}H-^{1}H *J*-resolved spectrum recorded on the same sample in 6 h using a data matrix of 2048 (t_2) × 256 (t_1) with 24 scans per t_1 increment. The relaxation delays were 1s. Data were processed using zero-filling up to 4096 (t_2) x 1024 (t_1) points and a sine filter in t_1. **(c)** Tilted SERF spectrum resulting from the application of semi-selective E-BURP excitation and RE-BURP refocusing pulses on the proton channel at $\upsilon_{2,3,7}$, with duration of 29.1 ms, corresponding to a frequency width of 170 Hz. Spectrum was recorded in 6 h using a data matrix of 2048 (t_2) × 256 (t_1) with 24 scans per t_1 increment. The relaxation delays were 1s. Data were processed using zero-filling up to 1024 points and a sine filter in t_1. Columns extractions corresponding to H_3 for both *J*-resolved and SERF spectra are also shown.

Table 1. Experimental dipolar couplings $D_{ij}^{\text{obs\_PBLG}}$ and AP-DPD calculated $D_{ij}^{\text{calc\_PBLG}}$ for the sample *t*-St/PBLG/THF-d_8. The $D_{ij}^{\text{obs\_ZLI}}$ determined from the analysis of ^{1}H NMR spectrum of *trans*-stilbene in ZLI1132 and the corresponding $D_{ij}^{\text{calc\_ZLI}}$ are also shown for comparison (adapted with permission from ref 10. Copyright 2012 American Chemical Society). Good agreement between AP-DPD-calculated and observed dipolar couplings implies a small RMS value

i, j	$D_{ij}^{\text{obs\_PBLG}}$(a) (Hz)	$D_{ij}^{\text{calc\_PBLG}}$(b) (Hz)	$D_{ij}^{\text{obs\_ZLI}}$(c) (Hz)	$D_{ij}^{\text{calc\_ZLI}}$(b) (Hz)
H−H couplings				
H_1,H_2			-4004.33 ± 0.03	-4004.85
H_1,H_3			-507.48 ± 0.06	-507.37
H_1,H_4			-1.48 ± 0.04	-0.69
H_1,H_5			247.46 ± 0.08	246.73
H_1,H_6			-2462.52 ± 0.08	-2462.51
H_1,H_7			-1732.91 ± 0.07	-1732.84
H_1,H_8			-397.17 ± 0.05	-399.16
H_1,H_9			-140.41 ± 0.04	-138.98
H_1,H_{10}			-104.60 ± 0.06	-103.64
H_2,H_3	9.7 ± 0.4	9.1	-20.45 ± 0.06	-19.85
H_2,H_4			246.98 ± 0.08	248.33
H_2,H_6	-1.4 ± 0.4	-1.2	-380.11 ± 0.09	-376.75
H_2,H_7	-1.4 ± 0.4	-0.9	-364.85 ± 0.09	-364.74
H_2,H_9			-64.74 ± 0.06	-63.36
H_2,H_{10}			-50.75 ± 0.06	-49.68
H_3,H_6	-1.1 ± 0.4	-1.0	-254.36 ± 0.14	-256.08
H_3,H_7	-1.1 ± 0.4	-0.7	-271.60 ± 0.14	-270.23
H_3,H_{10}			-39.58 ± 0.08	-39.82
H_6,H_7			681.36 ± 0.10	676.55
C−H couplings				
C_6,H_8	1.4 ± 0.6	1.1		
C_6,H_7	4.3 ± 0.7	4.4		
C_6,H_6	48.0 ± 0.4	48.1		
C_{13},H_1	6.8 ± 0.7	6.2		
C_5,H_1	1.5 ± 0.7	1.5		
C_5,H_5	27.5 ± 0.6	27.8		
C_4,H_2	1.4 ± 0.2	1.4		
C_4,H_4	27.4 ± 0.2	27.3		
C_3,H_1	-0.1 ± 0.6	-0.1		
C_3,H_3	-37.2 ± 0.6	-37.3		
RMS	0.35 Hz		1.67 Hz	

(a) calculated from $D_{ij}^{obs} = [\pm T_{ij}^{\text{PBLG}} - (\pm J_{ij}^{iso})]/2$.
(b) calculated *via* the AP-DPD method by using the software AnCon.
(c) extracted by using the software ARCANA (see ref 10).

Table 2. Values of the iteration parameters used in the conformational analysis with the AP-DPD approach of the *t*-St molecule dissolved in ZLI1132 and PBLG/THF-d_8. Adapted with permission from ref 10. Copyright 2012 American Chemical Society

	t-St in ZLI1132	*t*-St in PBLG/THF-d_8
$\phi_1^{max} = \pm\phi_2^{max}$ (degree)	16.80 ± 0.02	16.80 [(a)]
A_{C_2}	0.59 ± 0.01	0.59 [(a)]
$h_1 = h_2$ (degree)	10 (after parametrization)	10 [(a)]
$\varepsilon_{2,0}^{R}$ (RT)	1.349 ± 0.002	0.00388 ± 0.00003
$\varepsilon_{2,2}^{R}$ (RT)	0.650 ± 0.001	-0.00582 ± 0.00005
$\varepsilon_{2,0}^{H6-C=C-H7}$ (RT)	0.473 ± 0.006	0.00568 ± 0.00014
RMS (Hz)	1.67	0.35

[(a)] parameters fixed from conformational analysis in ZLI1132.

crystal. In the previous work [10], the set of 19 independent $D_{ij}^{\text{obs\_ZLI}}$ was fitted while iterating simultaneously on the interaction tensors $\varepsilon_{2,0}^{R}$, $\varepsilon_{2,2}^{R}$ and $\varepsilon_{2,0}^{H6-C=C-H7}$, the conformational terms $\phi_1^{max} = \pm\phi_2^{max}$, $h_1 = h_2$ and $A_{C_2} = 1 - A_{C_i}$, and the geometrical parameters of the *ene* group, until an acceptable RMS of 1.67 Hz. The single $D_{ij}^{\text{calc\_ZLI}}$ calculated by this approach are reported for comparison in the last column of Table 1, whereas the optimised values of the orientational and conformational terms are shown in Table 2. The surface $P_{iso}(\phi_1, \phi_2)$ resulting from this procedure is characterized by four symmetry related maxima of the probability function, corresponding to the C_2 (absolute maxima) and C_i (relative maxima) structures having, respectively, $\phi_1^{max} = \phi_2^{max}$ and $\phi_1^{max} = -\phi_2^{max}$, with $\phi_1^{max} = 16.8^\circ$ (Fig. 3). Hence, a first test is to verify whether or not the probability distribution

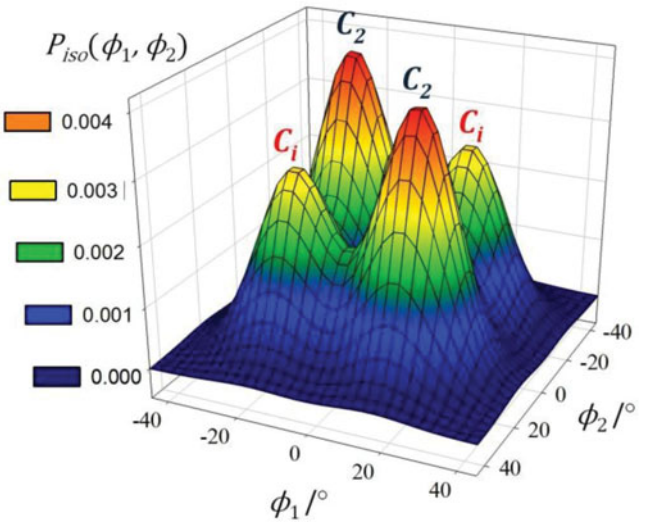

Figure 3. Experimental probability distribution $P_{iso}(\phi_1, \phi_2)$ for *t*-St dissolved in the nematic solvent ZLI1132 at 298 K. Reprinted with permission from ref 10. Copyright 2012 American Chemical Society.

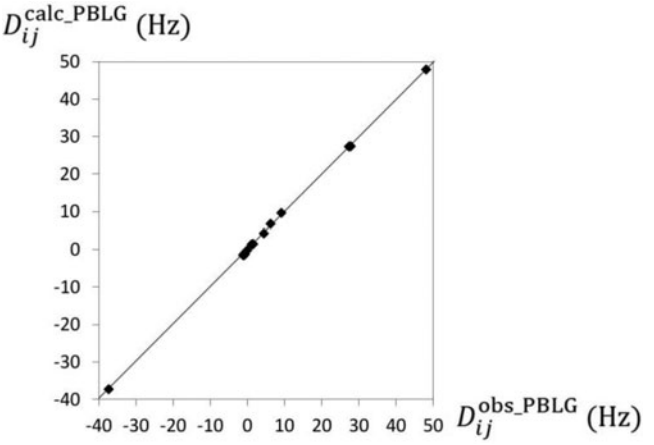

Figure 4. Observed *versus* theoretical dipolar couplings obtained for the *t*-St molecule dissolved in PBLG/THF-d_8, respectively from NMR experiments and by the AP-DPD approach.

obtained from the AP-DPD conformational analysis of *t*-St/ZLI1132 is still consistent with experimental data obtained for the same molecule in PBLG phase. Therefore, fixing the molecular geometry previously adjusted in ZLI1132 and keeping the terms $\phi_1^{max} = \pm\phi_2^{max}$, $h_1 = h_2$ and $A_{C_2} = 1 - A_{C_i}$ fixed at their optimized values for *t*-St/ZLI1132, the $\varepsilon_{2,0}^{R}$, $\varepsilon_{2,2}^{R}$ and $\varepsilon_{2,0}^{H6-C=C-H7}$ interaction tensor parameters were varied until the RMS error reached an acceptable value. As it can be appreciated in Fig. 4, the optimised values (Table 2) gave a good reproduction of $D_{ij}^{\text{obs\_PBLG}}$ with a low RMS of 0.35 Hz. The dipolar couplings $D_{ij}^{\text{calc\_PBLG}}$ calculated by this approach are reported, for comparison, in the third column of Table 1.

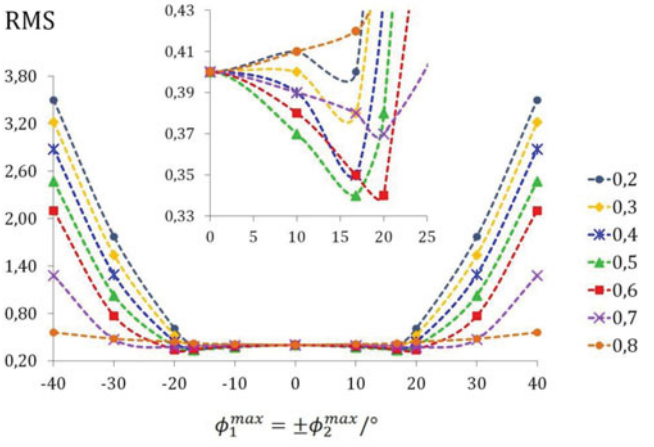

Figure 5. RMS value calculated for *t*-St in PBLG/THF-d_8 by the AP-DPD approach as a function of the torsion angles $\phi_1^{max} = \pm\phi_2^{max}$, while fixing the relative weight A_{C_2} at different values in the range 0.2–0.8 and $h_1 = 10^\circ$. The connecting lines are drawn as eye-guide.

The consistence of data in the thermotropic nematic and homopolypeptide lyotropic phases is a first satisfactory outcome. To further verify the meaningfulness of the experimental data collected in PBLG phase and to reach, if possible, a lower RMS, both conformational and orientational parameters have to be varied. Due to the small number of $D_{ij}^{\text{obs\_PBLG}}$ and/or their small values, it is mathematically unadvisable to iterate simultaneously on all the unknowns, in order to avoid false RMS minima. Hence, we parametrically changed the conformational terms, one by one, while iterating on $\varepsilon_{2,0}^{R}$, $\varepsilon_{2,2}^{R}$ and $\varepsilon_{2,0}^{H6-C=C-H7}$, and we followed the trend of the RMS target function. Figure 5 shows the RMS trend obtained by varying the torsion angle $\phi_1^{max} = \pm\phi_2^{max}$ from -40° to 40° for 7 different values of the relative weight A_{C_2}. The first evident feature is that all curves are basically flat between -20° and $+20^\circ$, whereas values of $|\phi_1^{max}| > 20^\circ$ do not reproduce adequately the $D_{ij}^{\text{obs\_PBLG}}$ and can be then immediately rejected. Some more details can be obtained by looking at the inset. For all curves, with the decrease of ϕ_1^{max} the RMS error decreases, reaches a minimum and then increases again to a fixed value of 0.40 at $\phi_1^{max} = 0^\circ$, corresponding to the full planar C_{2h} symmetry structure. Among all the sampled points, the best fit of the experimental data with an acceptably low RMS is obtained for $0.4 \leq A_{C_2} \leq 0.6$ and $10^\circ \leq \phi_1^{max} = \pm\phi_2^{max} \leq 20^\circ$ (fixing $h_1 = h_2 = 10^\circ$). This means that: (*i*) an equilibrium between the two couples of conformers has to be considered in order to reproduce the experimental data set with a low RMS, *i.e.* neither the couple of C_2 conformers nor that of C_i nor the single C_{2h} structure is sufficient alone to fit the D_{ij}^{obs}; (*ii*) situations with $0.4 \leq A_{C_2} \leq 0.6$ and $10^\circ \leq \phi_1^{max} \leq 20^\circ$ cannot be practically distinguished, since in these ranges not only RMS is acceptable but also the difference between each inter-ring $D_{ij}^{\text{obs\_PBLG}}$ and its corresponding $D_{ij}^{\text{calc\_PBLG}}$ is lower than 0.5.

Overall, the conformational analysis we performed on the sample *t*-St/PBLG/THF-d_8 does not individuate precise values for the twist angle of the most probable conformations and for their relative weight, but some restricted ranges are unambiguously determined. Such intervals are in perfect agreement with the conformational distribution obtained in ZLI1132. Therefore, it can be reasonably said that, when treatment in a thermotropic uniaxial solvent is not a viable way to obtain conformational information, the use of PBLG phases as alternative solvent can, together with the AP-DPD approach, yield meaningful results.

Orientational Results for *trans*-Stilbene in PBLG/THF-d_8 and Comparison with ZLI1132

Another point of this work deserves to be discussed in detail: analogies and differences between the orientational order experienced by *trans*-stilbene dissolved in ZLI1132 and in PBLG. Table 3 sums up the orientational order parameters found for *t*-St in the two phases (see Fig. 6 for the definition of the molecular axes). From them some interesting and somehow unexpected results can be deduced. Of course, *t*-St in ZLI1132 is much more ordered than in PBLG, so a direct comparison of the order parameters in terms of their values is inopportune and could be misleading. Nonetheless, looking at Table 3, we realize quite immediately that the two systems show common orientational features beside large differences, probably due to different orientational mechanisms experienced by the same probe-molecule in the two different media. First of all, it can be observed that the location of the PAS (Principal Axis System) for the Saupe matrix is roughly the same in two treated cases (Fig. 6): both the PAS's are reached by a simple rotation of the original $\{x, y, z\}$ molecular frame (where the vinyl group lies in the xz plane - with z along the double bond - and y is perpendicular to this plane, with its positive direction defined by

Table 3. Orientational order parameters found for *t*-St in ZLI1132 and PBLG/THF-d_8 mixture

	t-St in ZLI1132 [(a)]	*t*-St in PBLG/THF-d_8 [(b)]
S_{aa}	0.525	0.0019
$S_{bb} - S_{cc}$	0.174	−0.0024
S_{bb}	−0.176	−0.0021
S_{cc}	−0.350	0.0003
η (degree)	44.92	37.45

[(a)] Order parameters from ref. 10 for the C_2 conformer given in the PAS of the Saupe matrix for this conformation. The order parameters of the C_i conformer in the same molecular frame turned out to be essentially the same.
[(b)] Averaged order parameters for the C_2 and C_i conformers given in the PAS of the averaged Saupe matrix.

the right-handed rule) exclusively around y (*i.e.* a rotation on the xz plane) of an angle η, which is basically quite similar in the two cases ($\sim$37.5° for *t*-St/PBLG/THF-d_8 *vs* $\sim$45° for *t*-St/ZLI1132) and that leads the new z axis (now called a in the PAS) roughly along the long molecular axis. Looking at Table 3, we observe that the S_{aa} for both the situations has a positive value, then indicating a certain tendency of the long molecular axis to align along the director. However, the trend is different for the two other axes. For *t*-St in ZLI1132,

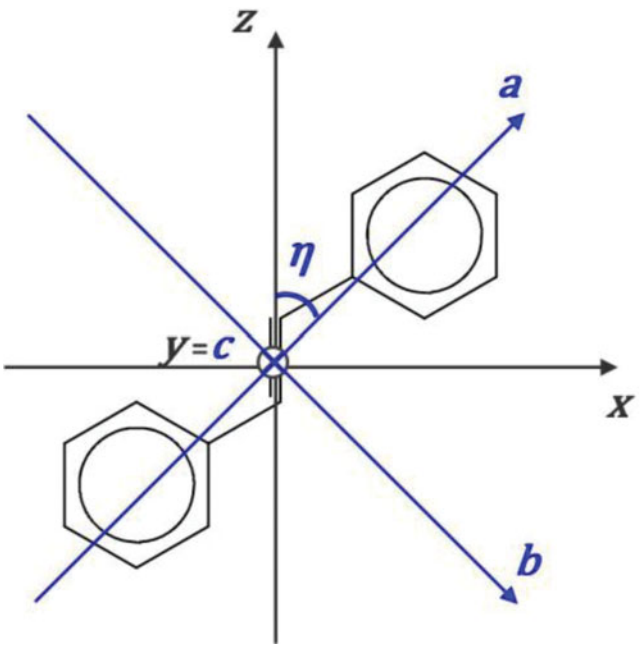

Figure 6. Definition of the original $\{x, y, z\}$ molecular frame and the $\{a, b, c\}$ molecular frame locating the principal axis system of the S matrix. The $\{a, b, c\}$ frame is obtained by an integral rotation of the $\{x, y, z\}$ frame of the angle η around y. The y and c axes, perpendicular to the (xz) and (ab) planes where the vinyl group lies, define right-handed Cartesian systems.

the quite high negative value of S_{cc} (-0.350) suggests a strong tendency of the c axis to be statistically oriented perpendicularly to the director, twice as much as the b axis ($S_{bb} = -0.176$). For *t*-St in the PBLG mesophase, on the contrary, there is a different statistical alignment of the axes b and c with respect to the director: the highest order parameter (in magnitude) is S_{bb} and it is negative, indicating a tendency of the b axis to be statistically oriented perpendicularly to the director. The very small value of S_{cc} means that c axis (very "rigidly" oriented of *t*-St/ZLI1132) randomly samples about all the possible orientations with about the same probability. This demonstrates that the short-range interactions, by now commonly recognized as the dominant orientational mechanism [2, 71–74] are substantially different for the two phases. In PBLG phase, in particular, the $S_{cc} \cong 0$ seems to indicate intuitively that the molecular tumbling about the a and b axes should be rather free (or at least less hindered), which is not the case in ZLI1132 nematic liquid crystal phase.

Conclusions

A comparative study of the conformational equilibrium and orientational order of *trans*-stilbene has been carried out for the first time by NMR spectroscopy in the weakly ordering phase made of PBLG dissolved in THF-d_8 and the highly ordering nematic ZLI1132 liquid crystal.

In both phases the AP-DPD treatment leads to a torsional surface characterized by four more stable symmetry-related conformations, that is a couple of global minima, where the molecule exhibits a propeller-like C_2 symmetry, and a couple of C_i local minima, where the rings are conrotated of the same angle. Data in thermotropic phase clearly individuate minimum conformers existing at $\phi_1^{max} = \phi_2^{max}$ (relative percentage of 59%) and $\phi_1^{max} = -\phi_2^{max}$ (relative percentage of 41%), with $\phi_1^{max} = 16.8^\circ$. In PBLG phase, due to the overlap of signals and/or symmetry of the structure, a reduced number of small residual dipolar couplings can be collected. This set individuates limited ranges where conformers are more probably confined, $10^\circ \leq \phi_1^{max} = \pm\phi_2^{max} \leq 20^\circ$ and $0.4 \leq A_{C_2} \leq 0.6$. The consistence between outcomes from the two mesophases testifies that conformational information derived from a weakly ordered sample is less accurate but reliable in individuating restricted intervals that contain the minimum energy conformers. This encourages the application of NMR in PBLG phase to the conformational study of more complex flexible molecules that are impossible to treat in a thermotropic phase and very difficult to study in solution by other techniques.

We also addressed the evaluation and relative comparison of the ordering features of the solute in the two phases. A naïve physical interpretation of the single principal order parameters intuitively suggests that the orientational interactions between the solute (roughly conceived as a "molecular platelet") and the PBLG or ZLI1132 mesophase molecules are basically different, particularly in the preferred geometry of the interactions.

Funding

The present work has been supported by the "L'Oréal Italia per le Donne e la Scienza" program through the fellowship of M. E. Di Pietro. Moreover, G. Celebre, G. De Luca and M. E. Di Pietro thank University of Calabria and MIUR PRIN 2009 for financial support.

References

[1] Saupe, A., & Englert, G. (1963). *Phys. Rev. Lett.*, *11*, 462–464.

[2] Celebre, G., De Luca, G., & Longeri, M. (2013). *eMagRes*, 335–350.
[3] Dong, R. (2012). *Encyclopedia of Analytical Chemistry*, John Wiley & Sons: New York.
[4] Emsley, J. W. (2007). *Encyclopedia of Magnetic Resonance*, John Wiley & Sons: New York.
[5] Chen, K., & Tjandra, N. (2012). In: *NMR of Proteins and Small Biomolecules.* Zhu, G. (Ed.), Chapter 3, Springer-Verlag: Berlin Heidelberg, 326.
[6] Jokisaari, J. (2011). *Encyclopedia of Magnetic Resonance*, John Wiley & Sons: New York.
[7] Burnell, E. E., & de Lange, C. A. (2003). *NMR of Ordered Liquids*, Kluwer Academic: Dordrecht, The Netherlands.
[8] Emsley, J. W. (1985). *Nuclear Magnetic Resonance of Liquid Crystals*, Reidel: Dordrecht, The Netherlands.
[9] Celebre, G., De Luca, G., & Di Pietro, M. E. (2013). *J. Mol. Struct.*, *1034*, 283.
[10] Celebre, G., De Luca, G., & Di Pietro, M. E. (2012). *J. Phys. Chem. B*, *116*, 2876.
[11] Celebre, G., De Luca, G., & Longeri, M. (2010). *Liq. Cryst.*, *37*, 923.
[12] Celebre, G., Concistré, M., De Luca, G., Longeri, M., Pileio, G., & Emsley, J. W. (2005). *Chem. Eur. J.*, *11*, 3599.
[13] Concistré, M., De Lorenzo, L., De Luca, G., Longeri, M., Pileio, G., & Raos, G. (2005). *J. Phys. Chem. A*, *109*, 9953.
[14] Celebre, G., De Luca, G., Longeri, M., Pileio, G., & Emsley, J. W. (2004). *J. Chem. Phys.*, *120*, 7075.
[15] Emsley, J. W., De Luca, G., Celebre, G., & Longeri, M. (1996). *Liq. Cryst.*, *20*, 569.
[16] Meerts, W. L., de Lange, C. A., Weber, A. C. J., & Burnell, E. E. (2009). *J. Chem. Phys.*, *139*, 044504.
[17] Meerts, W. L., de Lange, C. A., Weber, A. C. J., & Burnell, E. E. (2007). *Chem. Phys. Lett.*, *441*, 324.
[18] Kummerlöwe, G., & Luy, B. (2009). *Trends Anal. Chem.*, *28*, 483.
[19] Thiele, C. M. (2008). *Eur. J. Org. Chem.*, 5673.
[20] Thiele, C. M. (2007). *Conc. Magn. Reson. Part A*, *30*, 65.
[21] Bax, A., & Grishaev, A. (2005). *Curr. Opin. Struct. Biol.*, *15*, 563.
[22] Prestegard, J. H., Bougault, C. M., & Kishore, A. I. (2004). *Chem. Rev.*, *104*, 3519.
[23] Suryaprakash, N. (1998). *Concepts Magn. Reson.*, *10*, 167.
[24] Courtieu, J., Lesot, P., Meddour, A., Merlet, D., & Aroulanda, C. (2002). *Encyclopedia of NMR: Advances in NMR*, *9*, 497.
[25] Aroulanda, C., Sarfati, M., Courtieu, J., & Lesot, P. (2001). *Enantiomer*, *6*, 281.
[26] Sarfati, M., Lesot, P., Merlet, D., Courtieu, J. (2000). *Chem. Commun.*, 2069.
[27] Samulski, E. T., Tobolski, A. V. (1968). *Macromolecules*, *1*, 555.
[28] Di Pietro, M. E., Aroulanda, C., Merlet, D., Celebre, G., & De Luca, G. (2014). *J. Phys. Chem. B*, *118*, 9007.
[29] Lesot, P., Serhan, Z., & Billault, I. (2011). *Anal. Bioanal. Chem.*, *399*, 1187.
[30] Marx, A., Böttcher, B., & Thiele, C. M. (2010). *Chem. Eur. J.*, *16*, 1656.
[31] Aroulanda, C., Lafon, O., & Lesot, P. (2009). *J. Phys. Chem. B*, *113*, 10628.
[32] Thiele, C. M. (2004). *J. Org. Chem.*, *69*, 7403.
[33] Lesot, P., Sarfati, M., & Courtieu, J. (2003). *Chem. Eur. J.*, *9*, 1724.
[34] O'Hagan, D., Goss, R. J. M., Meddour, A., & Courtieu, J. (2003). *J. Am. Chem. Soc.*, *125*, 379.
[35] Thiele, C. M., & Berger, S. (2003). *Org. Lett.*, *5*, 705.
[36] Aroulanda, C., Boucard, V., Guibé, F., Courtieu, J., & Merlet, D. (2003). *Chem. Eur. J.*, *9*, 4536.
[37] Rivard, M., Guillen, F., Fiaud, J.-C., Aroulanda, C., & Lesot, P. (2003). *Tetrahedron: Asymmetry*, *14*, 1141.
[38] Villar, H.; Guibé, F., Aroulanda, C., & Lesot, P. (2002). *Tetrahedron: Asymmetry*, *13*, 1465.
[39] Péchiné, J.-M., Meddour, A., & Courtieu, J. (2002). *Chem. Commun.*, 1734.
[40] Canlet, C., Merlet, D., Lesot, P., Meddour, A., Loewenstein, A., & Courtieu, J. (2000). *Tetrahedron: Asymmetry*, *11*, 1911.
[41] Giraud, N., Beguin, L., Courtieu, J., & Merlet, D. (2010). *Angew. Chem. Int. Ed.*, *49*, 3481.
[42] Kobzar, K., & Luy, B. (2007). *J. Magn. Reson.*, *186*, 131.

[43] Furrer, J., John, M., Kessler, H., & Luy, B. (2007). *J. Biomol. NMR*, *37*, 231.
[44] Tzvetkova, P., Simova, S., & Luy, B. (2007). *J. Magn. Reson.*, *186*, 193.
[45] Kim, N., Kim, J. K., Hwang, D., & Lim, Y. H. (2013). *Med. Mycol.*, *51*, 45.
[46] Piotrowska, H., Kucinska, M., & Murias, M. (2012). *Mutat. Res.*, *750*, 60.
[47] Belluti, F., Fontana, G., Dal Bo, L., Carenini, N., Giommarelli, C., & Zunino, F. (2010). *Bioorgan. Med. Chem.*, *18*, 3543.
[48] Hong, M. C., Kim, Y. K., Choi, J. Y., Yang, S. Q., Rhee, H., Ryu, Y. H., Choi, T. H., Cheon, G. J., An, G. I., Kim, H. Y., *et al.* (2010). *Bioorg. Med. Chem.*, *18*, 7724.
[49] Milne, J. C., Lambert, P. D., Schenk, S., Carney, D. P., Smith, J. J., Gagne, D. J., Jin, L., Boss, O., Perni, R. B., Vu, C. B., *et al.* (2007). *Nature*, *450*, 712.
[50] Balan, K. V., Wang, Y., Chen, S. W., Chen, J.-C., Zheng, L.-F., Yang, L., Liu, Z.-L., Pantazis, P., Wyche, J. H., Han, Z. (2006). *Biochem. Pharmacol.*, *72*, 573.
[51] Olas, B., & Wachowicz, B. (2005). *Platelets*, *16*, 251.
[52] Bhat, K. P. L., Lantvit, D., Christov, K., Mehta, R. G., Moon, R. C., & Pezzuto, J. M. (2001). *Cancer Res.*, *61*, 7456.
[53] Bowers, J. L., Tyulmenkov, V. V., Jernigan, S. C., & Klinge, C. M. (2000). *Endocrinology*, *141*, 3657.
[54] Maccarrone, M., Lorenzon, T., Guerrieri, P., Finazzi Agrò, A. (1999). *Eur. J. Biochem.*, *265*, 27.
[55] Jang, M., Cai, L., Udeani, G. O., Slowing, K. V., Thomas, C. F., Beecher, C. W. W., Fong, H. H., Farnsworth, N. R., Kinghorn, A. D., Mehta, R. G., *et al.* (1997). *Science*, *275*, 218.
[56] Tomatsu, I., Peng, K., & Kros, A. (2011). *Adv. Drug Delivery Rev.*, *63*, 1257.
[57] Meng, F., Zhong, Z., & Feijen, J. (2009). *Biomacromolecules*, *10*, 197.
[58] Zoppi, L., Calzolari, A., Ruini, A., Ferretti, A., & Caldas, M. (2008). *Phys. Rev. B*, *78*, 165204.
[59] Buruiana, E. C., Zamfir, M., & Buruiana, T. (2007). *Eur. Polym. J.*, *43*, 4316.
[60] Emsley, J. W., Luckhurst, G. R., & Stockley, C. P. (1982). *Proc. R. Soc. London, Ser. A*, *381*, 117.
[61] Celebre, G., De Luca, G., Emsley, J. W., Foord, E. K., Longeri, M., Lucchesini, F., & Pileio, G. (2003). *J. Chem. Phys.*, *118*, 6417.
[62] Emsley, J. W., Lesot, P., Merlet, D. (2004) *Phys. Chem. Chem. Phys.*, *6*, 522.
[63] Emsley, J. W., Lesot, P., Courtieu, J., & Merlet, D. (2004) *Phys. Chem. Chem. Phys.*, *6*, 5331.
[64] De Luca, G., Longeri, M., Pileio, G., & Lantto, P. (2005). *Chem. Phys. Chem.*, *6*, 2086.
[65] Celebre, G., & De Luca, G. (2003). *J. Phys. Chem. B*, *107*, 3243.
[66] Celebre, G., & Longeri, M. (2003). In: *NMR of Ordered Liquids*, Burnell, E. E. & de Lange, C. A. (Eds.), Chapter 14, Kluwer Academic: Dordrecht, The Netherlands, 305.
[67] Pileio, G. (2005). Ph.D. Thesis, Università della Calabria, Italy.
[68] Diehl, P. (2007). *Encyclopedia of Magnetic Resonance*, John Wiley & Sons: New York.
[69] Vaara, J., Jokisaari, J., Wasylishen, R. E., & Bryce, D. L: (2002). *Prog. Nucl. Magn. Reson. Spectrosc.*, *41*, 233.
[70] Fäcke, T., & Berger, S. (1995). *J. Magn. Reson. Ser. A*, *113*, 114.
[71] Celebre, G., & De Luca, G. (2003). *J. Phys. Chem. B*, *107*, 3243.
[72] Celebre, G., & De Luca, G. (2003). *Chem. Phys. Lett.*, *368*, 359.
[73] Celebre, G. (2001). *J. Chem. Phys.*, *115*, 9552.
[74] Celebre, G. (2001). *Chem. Phys. Lett.*, *342*, 375.